Am J Transl Res 2024;16(7):2828-2839
www.ajtr.org /ISSN:1943-8141/AJTR0156835

Original Article

Identification of prognostic biomarkers for hepatocellular carcinoma with vascular invasion

Lei Sun*, Chen Fan, Ping Xu, Fei-Hu Sun, Hao-Huan Tang, Wei-Dong Wang*

*Department of Interventional Radiology, The Affiliated Wuxi People's Hospital of Nanjing Medical University, Wuxi People's Hospital, Wuxi Medical Cencer, Nanjing Medical University, Wuxi 214000, Jiangsu, China. *Equal contributors.*

Received March 27, 2024; Accepted May 20, 2024; Epub July 15, 2024; Published July 30, 2024

Abstract: Objective: Vascular invasion (VI) profoundly impacts the prognosis of hepatocellular carcinoma (HCC), yet the underlying biomarkers and mechanisms remain elusive. This study aimed to identify prognostic biomarkers for HCC patients with VI. Methods: Transcriptome data from primary HCC tissues and HCC tissues with VI were obtained through the Genome Expression Omnibus database. Differentially expressed genes (DEGs) in the two types of tissues were analyzed using functional enrichment analysis to evaluate their biological functions. We examined the correlation between DEGs and prognosis by combining HCC transcriptome data and clinical information from The Cancer Genome Atlas database. Univariate and multivariate Cox regression analyses, along with the least absolute shrinkage and selection operator (LASSO) method were utilized to develop a prognostic model. The effectiveness of the model was assessed through time-dependent receiver operating characteristic (ROC) curve, calibration diagram, and decision curve analysis. Results: In the GSE20017 and GSE5093 datasets, a total of 83 DEGs were identified. Gene Ontology analysis indicated that these DEGs were predominantly associated with xenobiotic stimulus, collagen-containing extracellular matrix, and oxygen binding. Additionally, Kyoto Encyclopedia of Genes and Genomes analysis revealed that the DEGs were primarily involved in immune defense and cellular signal transduction. Cox and LASSO regression further identified 7 genes (HSPA8, ABCF2, EAF1, MARCO, EPS8L3, PLA3G1B, C6), which were used to construct a predictive model in the training cohort. We used X-tile software to calculate the optimal cut-off value to stratify HCC patients into low-risk and high-risk groups. Notably, the high-risk group exhibited poorer prognosis than the low-risk group ($P < 0.001$). The model demonstrated area under the ROC curve (AUC) values of 0.815, 0.730, and 0.710 at 1-year, 3-year, and 5-year intervals in the training cohort, respectively. In the validation cohort, the corresponding AUC values were 0.701, 0.571, and 0.575, respectively. The C-index of the calibration curve for the training and validation cohorts were 0.716 and 0.665. Decision curve analysis revealed the model's efficacy in guiding clinical decision-making. Conclusions: The study indicates that 7 genes may be potential prognostic biomarkers and treatment targets for HCC patients with VI.

Keywords: Hepatocellular carcinoma, vascular invasion, prognostic model

Introduction

Hepatocellular carcinoma (HCC) is a predominant form of liver cancer and the third leading cause of cancer-related mortality worldwide [1]. HCC is distinguished by its highly vascular and infiltrative nature, particularly its propensity for vascular invasion (VI). VI in HCC encompasses macrovascular invasion (macro VI) and microvascular invasion (micro VI). Macro VI is characterized by the infiltration of the tumor into major blood vessels, including the main portal vein and its branches, the hepatic vein and its branches, or the inferior vena cava. Detection of macro VI can be achieved through macroscopic examinations or radiological imaging. In advanced HCC, the emergence of macro VI is identified as a significant prognostic indicator, suggesting an unfavorable outcome [2]. Macro VI has been integrated into the Barcelona Clinic Liver Cancer staging systems, aiding the selection of optimal treatment approaches for HCC [3]. On the other hand, micro VI is characterized by the presence of cancer cells within the vascular lumen lined by endothelial cells, necessitating microscope detection [4]. This manifestation serves as an independent risk factor for tumor recurrence following liver transplantation or hepatectomy [5].

https://doi.org/10.62347/SQZW3775

The presence of VI in HCC is a crucial factor in determining appropriate treatment strategies. In cases where VI is present, a more comprehensive and aggressive approach is necessary, which may include surgical resection, interventional therapy, and a combination of systemic targeted and immunotherapy. While advancements in medical imaging have improved the detection of macro VI, the identification of micro VI remains challenging and often requires post-surgical pathological examination of resected tissue sections. Hence, identification of reliable molecular biomarkers for VI in HCC and precise prediction of tumor recurrence are crucial for the management of this disease. Mínguez conducted a genome-wide gene expression analysis on 79 samples of HCC, revealing a distinct gene expression signature comprising 35 genes linked to VI in HCC [6]. Budhu identified 17 genes through a study involving 9 HCC samples, serving as predictors for HCC venous metastasis [7].

HCC with VI presents a therapeutic challenge, necessitating the development of a more robust and precise predictive model to inform clinical decision-making. This study seeks to identify gene signatures linked to in HCC patients with VI by integrating transcriptional data from a substantial number of HCC samples in the Genome Expression Omnibus (GEO) and The Cancer Genome Atlas (TCGA) databases. A comprehensive predictive prognosis model, centered on VI-related genes, was established, contributing to a theoretical foundation for personalized treatment strategies and novel therapeutic targets for HCC.

Methods

Data collection

The GSE20017 and GSE5093 datasets were sourced from the GEO database (https://www.ncbi.nlm.nih.gov/geo/), with a total of 135 and 20 samples, respectively. Within the GSE20017 dataset, there were 95 cases of HCC and 40 cases of HCC with VI, while the GSE5093 dataset contained 11 cases of HCC and 9 cases of HCC with VI. Furthermore, transcriptome data and clinical information of 374 HCC samples were retrieved from TCGA database (https://cancergenomes.nih.gov/).

Identification of differentially expressed genes (DEGs)

The GEO2R tool (https://www.ncbi.nlm.nih.gov/geo/geo2r/) [8] was utilized to analyze the GSE20017 and GSE5093 datasets in order to and identify DEGs, with selection criteria of |log2 (FC)| > 1 and adj. $P < 0.05$.

Functional enrichment analysis of DEGs

Gene Ontology (GO) analysis and Kyoto Encyclopedia of Genes and Genomes (KEGG) pathway enrichment analysis were performed on the DEGs. Pathways and biological processes meeting the significance threshold of $P < 0.05$ and $q < 0.05$ were identified for further analysis.

Development of the prognostic model

In order to assess the relationship between DEGs and patient prognosis, we conducted univariate Cox, LASSO, and multivariate Cox analyses on the downloaded TCGA data. The TCGA cohort was randomly split into a training cohort (n = 259) and a validation cohort (n = 211) at a ratio of 7:3 using the "createDataPartition" function within the "caret" package to develop a prognostic model. Initially, we utilized the "survival" package to perform univariate Cox regression analysis, identifying DEGs with a significance level of $P < 0.05$. LASSO regression analysis was employed to enhance the results, followed by multivariate Cox regression analysis using the "coxph" function to develop a multivariate Cox proportional hazard model. The independent prognostic genes identified in the multivariate Cox regression analysis were employed to generate a nomogram through the "nomogram" function. The risk score for each sample was determined using the following formula:

$$Riskscore = \sum_{i=1}^{n} (coef_i \times x_i).$$

Within this formula, $Coef_i$ represents the cooperativity coefficient, while x_i denotes the relative gene expression that has been standardized by Z-score.

Evaluation of the prognostic model

Receiver operating characteristic (ROC) curves were utilized in the training cohort to assess

the discriminatory capacity of the prognostic model. Calibration curves were evaluated through 800 bootstrap resampling to determine the degree of fit between predicted and observed survival rates at 1-year, 3-year, and 5-year intervals. The precision of the nomogram was examined using decision curve analysis (DCA) at 1-year, 3-year, and 5-year intervals, with the plots created using the "ggDCA" package. DCA was utilized to assess the clinical utility of the prognostic model in informing clinical decision-making. The validation cohort also underwent similar evaluation using the same parameters.

Identification of independent prognostic factors for HCC

To investigate the correlation between HCC prognosis and different clinical variables, including the risk score, we performed univariate and multivariate Cox regression analyses in both the training and validation cohorts.

Relationships of the prognostic IV-related signature with immune cell infiltration

We further explored the relationship between the prognostic model and immune cell infiltration in HCC. Utilizing the online database Tumor Immune Estimation Resource (TIMER), which provide a comprehensive platform for evaluating the clinical relevance of diverse immunocytes in various cancer types, we were able to analyze and visualize the levels of tumor-infiltrating immunocytes [9]. Specifically, we retrieved the immune infiltrating levels of HCC patients, and subsequently assessed the associations between these levels and our prognostic signature.

Comparison analysis of immune checkpoints expression in high and low risk groups

Immunotherapy has become an important anticancer approach for a significant number of malignant tumors, with a goal of improving prognosis. In this study, we further investigated the expression levels of prevalent immune checkpoints in both high and low-risk HCC patients.

Statistical methods

The X-tile software was employed to determine the optimal cut-off value of the risk score, leading the stratification of patients into high- and low-risk categories. Survival curves were generated using Kaplan Meier method, and log rank test was utilized to compare survival outcomes between the two groups. All statistical analyses were conducted using R version 4.2.2, with a significance level set at $P < 0.05$. Pearson correlation analysis was utilized to assess relationships between variables.

Results

Identification of DEGs in primary HCC and HCC with VI

A total of 14 DEGs were identified in the GSE20017 dataset, while 69 DEGs were found in the GSE5093 dataset (**Figure 1A**, **1B**). There was no overlap of DEGs between the two datasets. The total 83 DEGs associated with VI included 12 upregulated ones and 71 downregulated ones.

Functional enrichment analysis of DEGs

The top 3 biological processes identified were response to xenobiotic stimulus, cellular response to xenobiotic stimulus, and long-chain fatty acid transport. The top 3 cellular components included collagen-containing extracellular matrix, secretory granule lumen, and cytoplasmic vesicle lumen. The identified molecular functions were oxygen binding, collagen binding, and laminin binding (**Figure 2A**). Additionally, KEGG pathway enrichment analysis revealed significant pathways, such as phagosome, focal adhesion, and complement and coagulation cascades (**Figure 2B**).

Establishment of prognostic model in the TCGA training cohort

In the training cohort, univariate Cox regression analysis was performed on 83 DEGs, which revealed correlations between 25 genes and the overall survival (OS) of HCC (**Figure 3A**). Through the use of LASSO regression, 12 key genes namely, HSPA8, CYP3A5, ABCF2, TROAP, EAF1, MARCO, LDHA, ACTG1, EPS8L3, PLA2G1B, C6, and HNRNPH1, were identified (**Figure 3B**, **3C**). Subsequent multivariate Cox regression analysis further narrowed down to a list of 7 genes that significantly influence prognosis: HSPA8, ABCF2, EAF1, MARCO, EPS8L3, PLA3G1B, and C6 (**Figure 4A**). Finally, a prognostic model was developed utilizing the 7 genes, with the risk score equals to HSPA8 * 0.003 + ABCF2 * 0.078 + EAF1 *

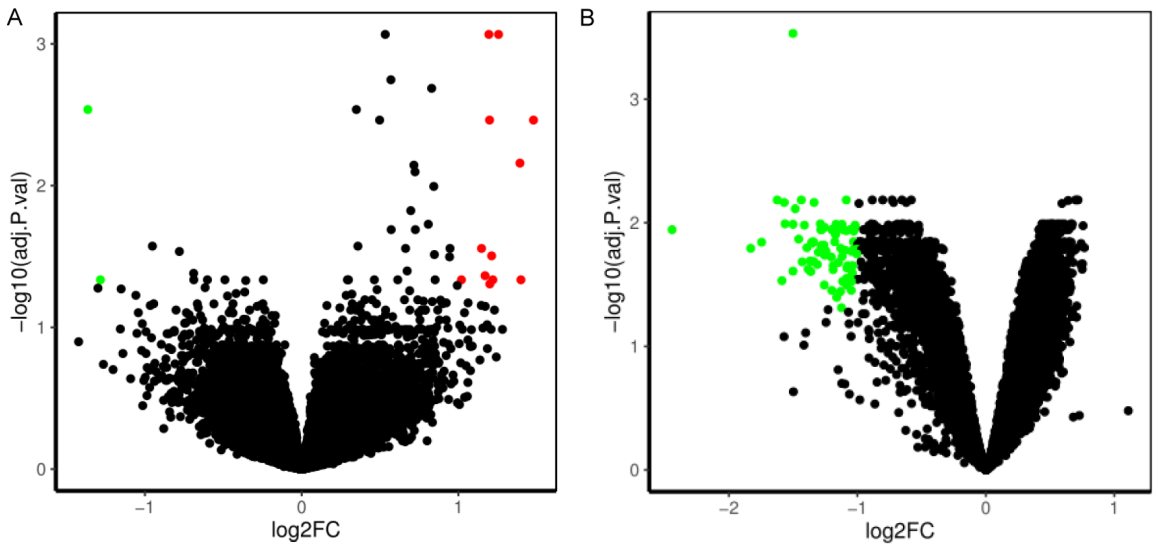

Figure 1. Volcanic maps of the DEGs in primary HCC and HCC with VI. A: DEGs in the GSE20017. B: DEGs in the GSE5093. In both maps, red or green dots represent genes that are up- or down-regulated in HCC with VI compared to primary HCC tissues, respectively. Gray dots represent genes that showed no significant difference in expression between the two tissue types.

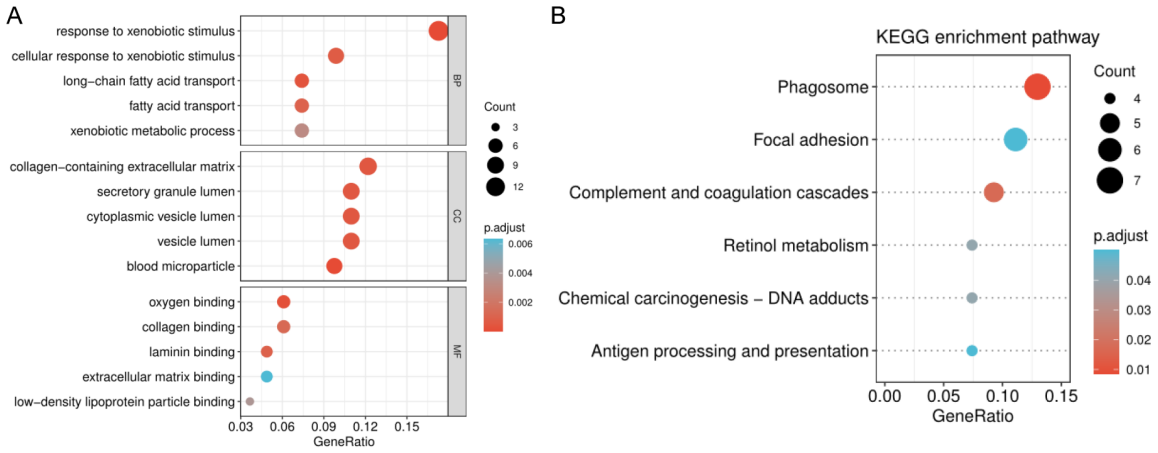

Figure 2. Function enrichment analysis of DEGs. A: GO analysis. B: KEGG analysis.

0.104 + MARCO * 0.040 + EPS8L3 * 0.025 + PLA2G1B * 0.057 + C6 * -0.005. A nomograph was then generated to visually represent this model (**Figure 4B**). The optimal cut-off value for risk score, determined by X-tile software, was found to be 2.43, which was used for the classification of patients into low-risk and high-risk groups. Following the Kaplan-Meier survival analysis, a significant disparity in OS was observed between the high-risk and low-risk groups ($P < 0.001$) (**Figure 5A**). The discriminatory performance of the model was evaluated using a time-dependent ROC curve. In the training cohort, the area under the curve (AUC) for the predicted 1-year, 3-year, and 5-year survival rates were 0.815, 0.730, and 0.710, respectively (**Figure 6A**). These findings indicate that the model exhibits a favorable predictive capacity. The calibration plot of the training cohort exhibited strong concordance between predicted and observed survival rates (**Figure 7A**). The C-index for predicting OS was 0.716 (95% CI, 0.688 to 0.744). Moreover, DCA for 1-year, 3-year, and 5-year survival rates indicated that the model's favorable clinical utility in guiding clinical decision-making (**Figure 8A**).

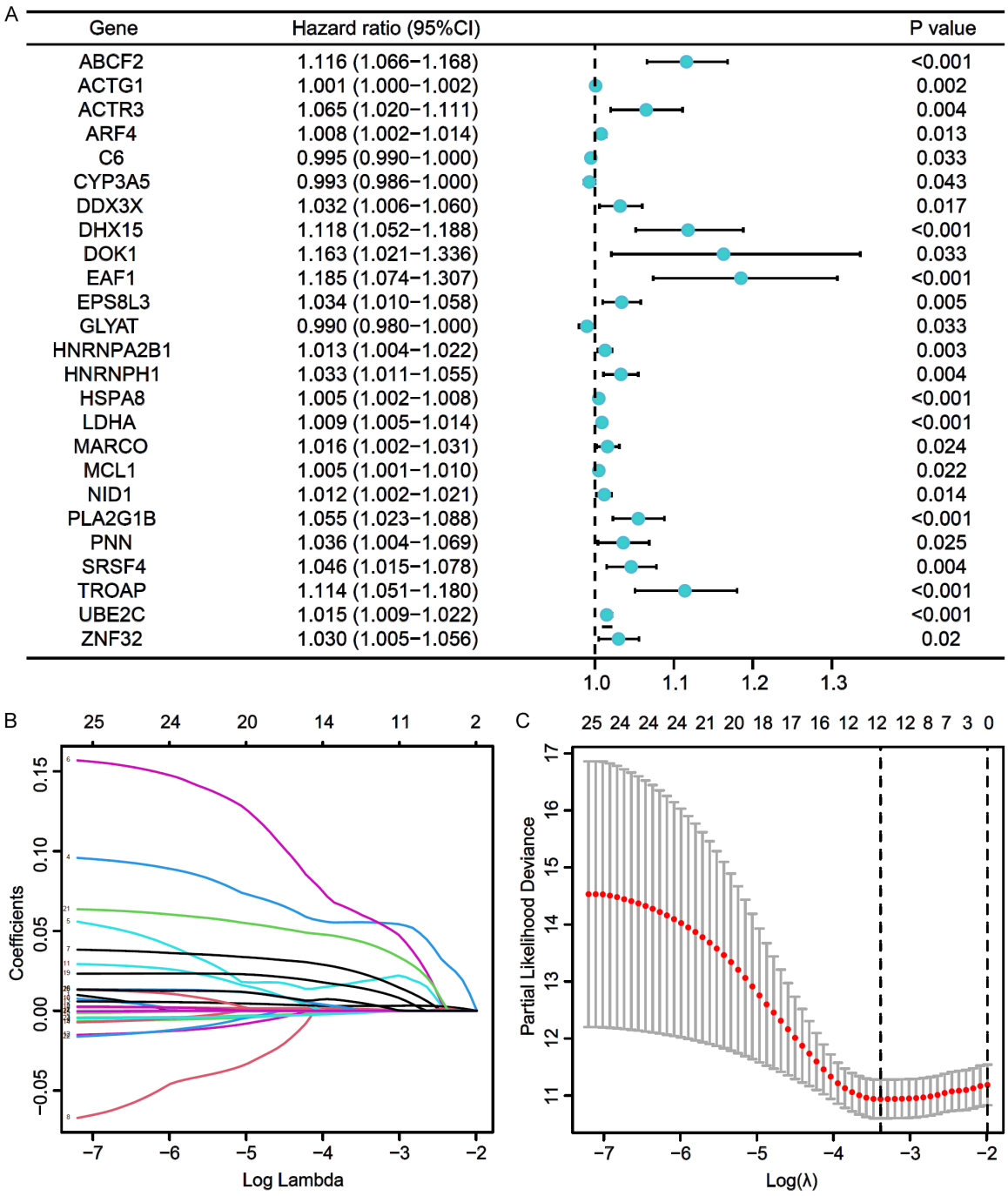

Figure 3. A: Screening of prognostic genes by univariable Cox analysis. B and C: The LASSO regression analysis identified 12 key genes.

Validation of the prognostic model in the TCGA validation cohort

In order to assess the predictive capability of the prognostic model, the validation dataset was utilized to stratify patients into low-risk and high-risk groups based on the predetermined cut-off value of 2.43. The OS of patients in the low-risk group was found to be significantly longer than that of the high-risk group ($P < 0.001$) (**Figure 5B**). The AUC values for the model's predicted 1-year, 3-year, and 5-year survival rates were 0.701, 0.571 and 0.575, respectively (**Figure 6B**), suggesting the reliability of the

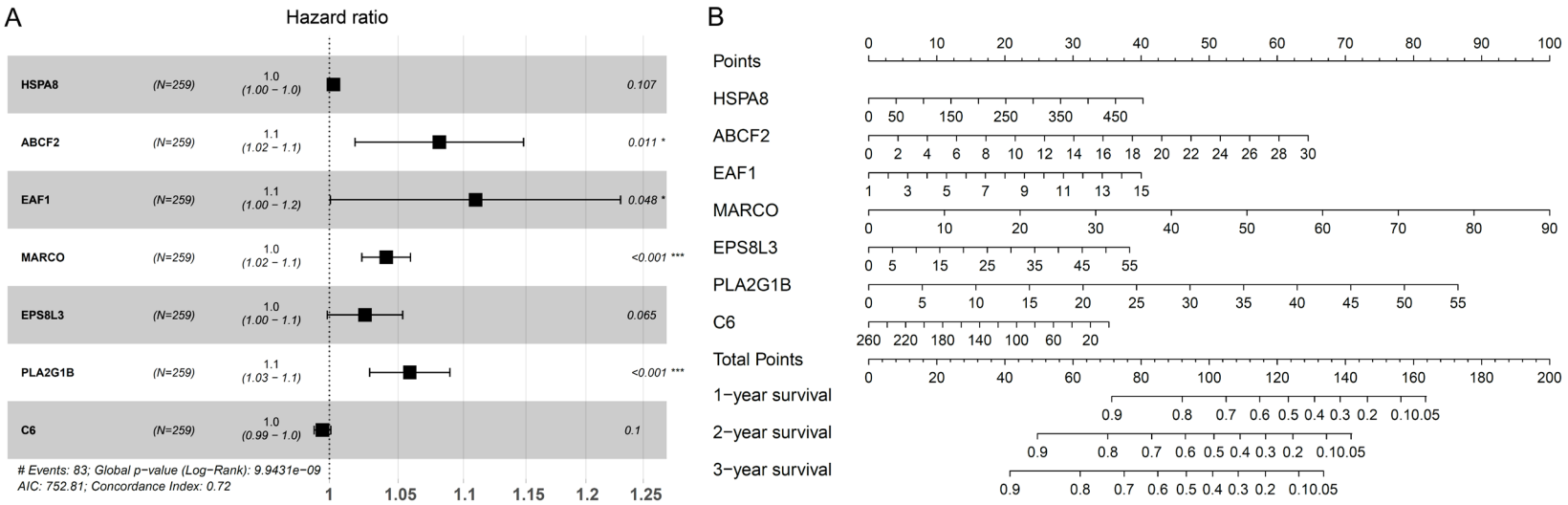

Figure 4. A: Forest maps of 7 genes in multivariable Cox regression model. B: Prognostic nomogram based on the 7 genes.

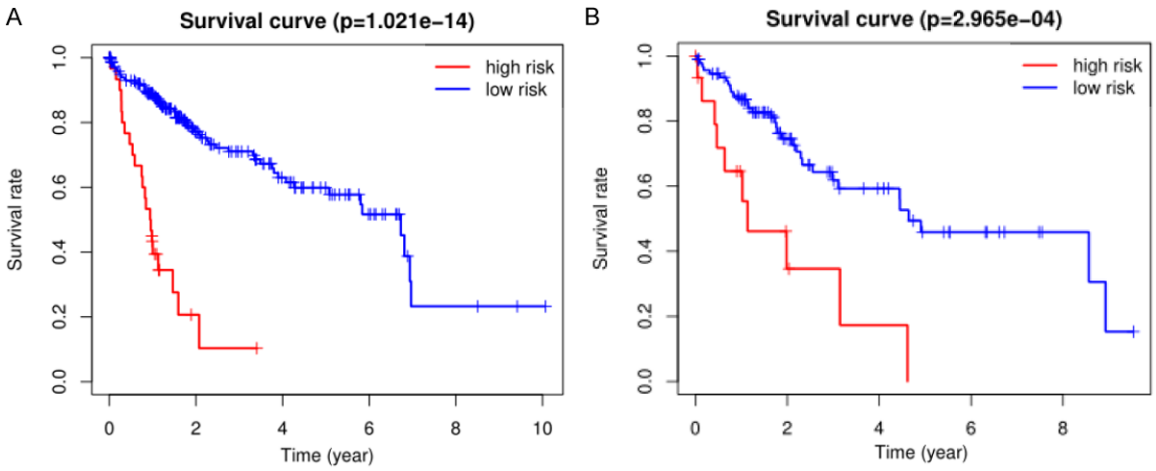

Figure 5. Survival analysis curves. A: Training cohort. B: Validation cohort.

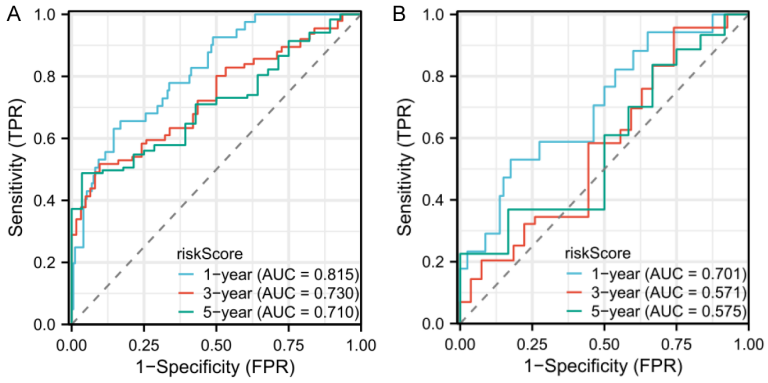

Figure 6. Time dependent ROC curves. A: Training cohort. B: Validation cohort.

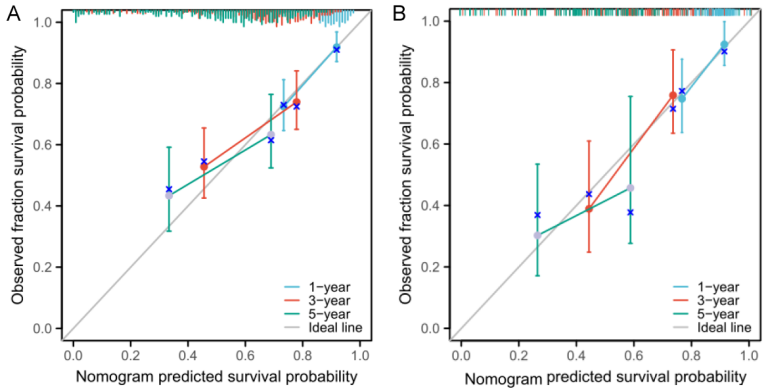

Figure 7. 1-year, 3-year, and 5-year calibration curves. A: Training cohort. B: Validation cohort.

model. The C-index for OS prediction was calculated to be 0.665 (95% CI, 0.615 to 0.716) (**Figure 7B**). Furthermore, we plotted the DCA curve for 1-year, 3-year, and 5-year intervals (**Figure 8B**).

Efficacy assessment of the prognostic risk model

Univariate and multivariate Cox regression analyses revealed that the risk score could serve as an independent risk factor influencing the prognosis of HCC in both the training and validation cohorts (**Figure 9A-D**).

Different immune infiltrating levels in high- and low-risk groups in e thTCGA training cohort

The relationship between the prognostic signature associated with VI and the immunocytes infiltration in HCC was estimated to examine the potential of risk score in reflecting the status of the tumor immune microenvironment. The results showed that a significant increase in neutrophil (Cor = 0.268, *P* = 1.272e-05), macrophage (Cor = 0.243, *P* = 8.011e-5) and dendritic cell (Cor = 0.210, *P* =0.001) counts in high-risk patients (**Figure 10A-C**), indicating distinct immune statuses between high- and low-risk groups. Additionally, CD8 T cells (Cor = 0.131, *P* = 0.035) also exhibited a correlation with high risk (**Figure 10D**). The levels of B cells and CD4 T cells did not exhibit

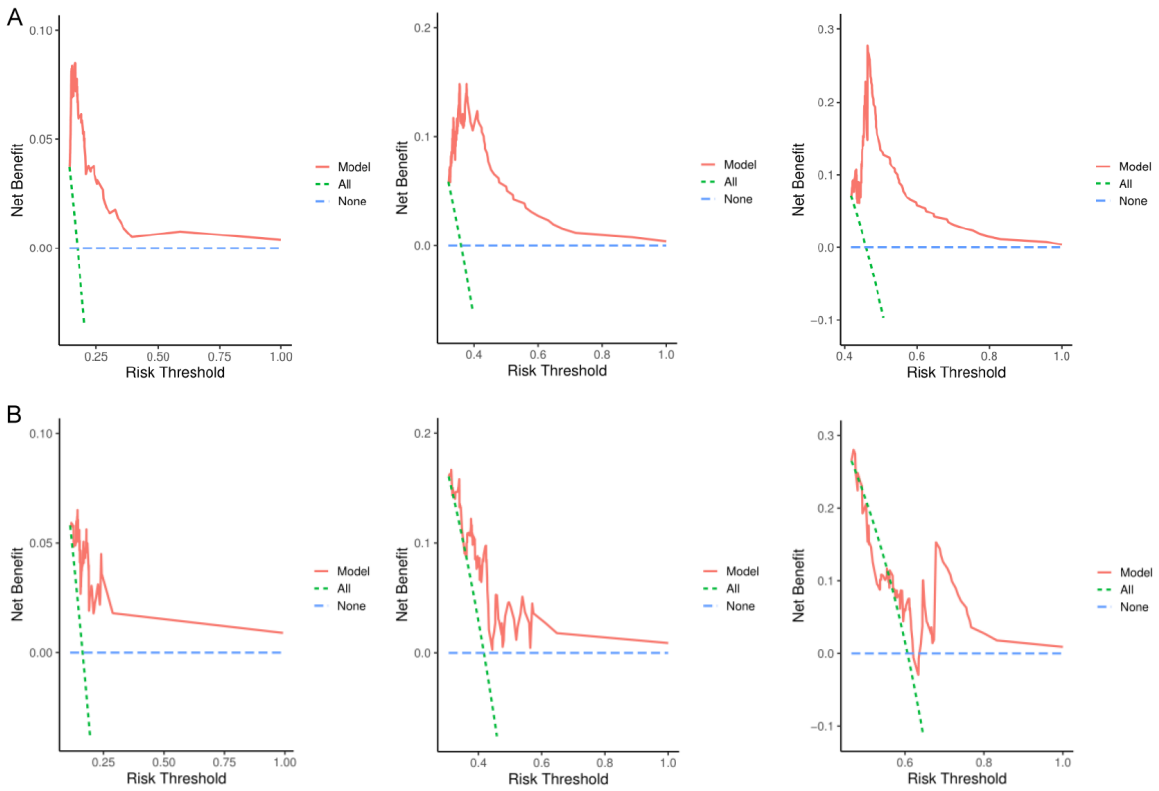

Figure 8. 1-year, 3-year and 5-year DCA curves. A: Training cohort. B: Validation cohort.

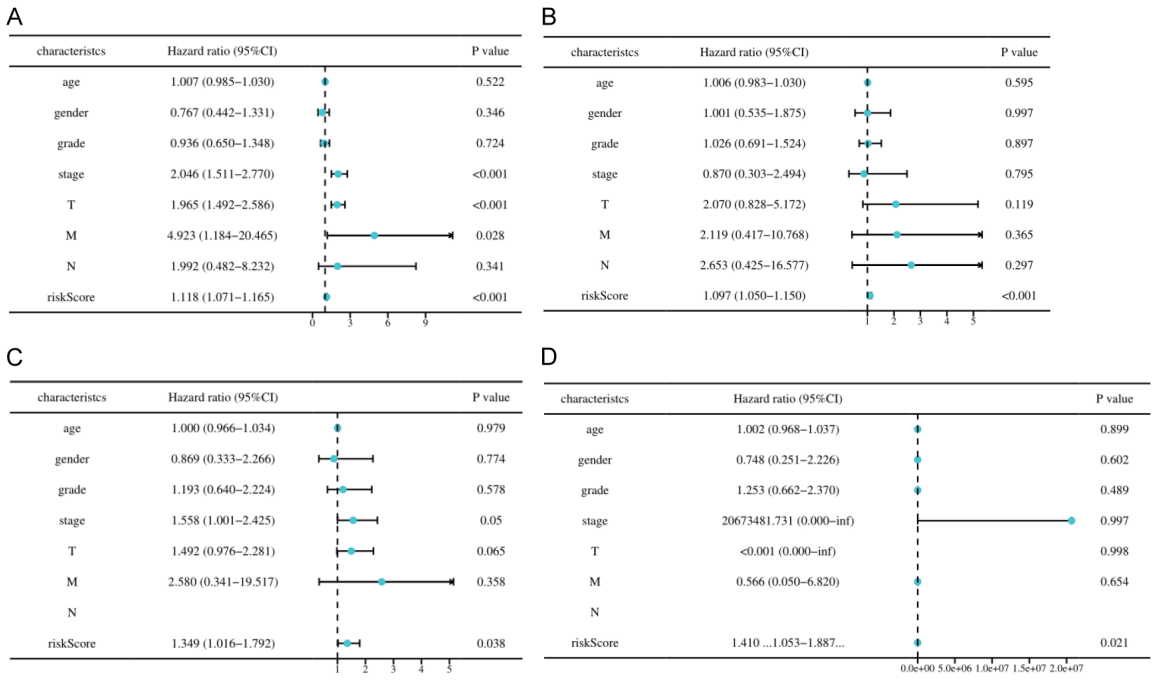

Figure 9. Forest plot of univariate and multivariate Cox regression analysis. A and B: Training cohort. C and D: Validation cohort.

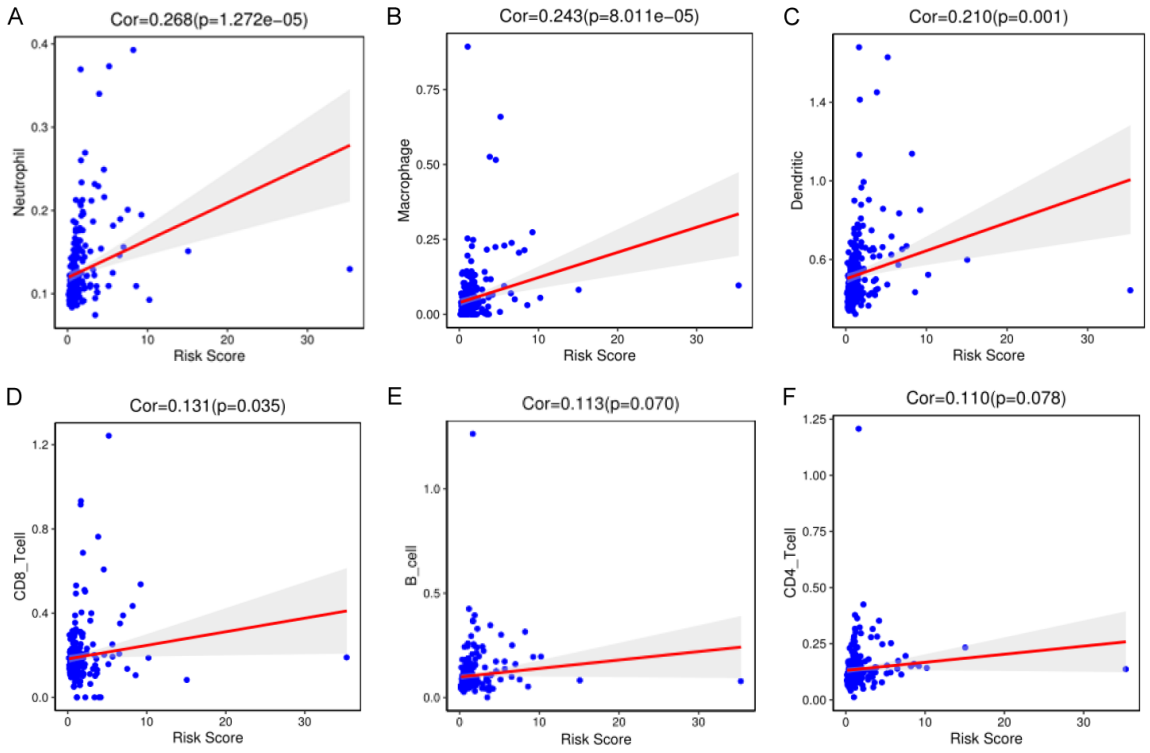

Figure 10. Relationships between the IV-related prognostic model and infiltration abundances of six types of immune cells. A: Neutrophil. B: Macrophage. C: Dendritic cells. D: CD8+ T cells. E: B cells. F: CD4+ T cells.

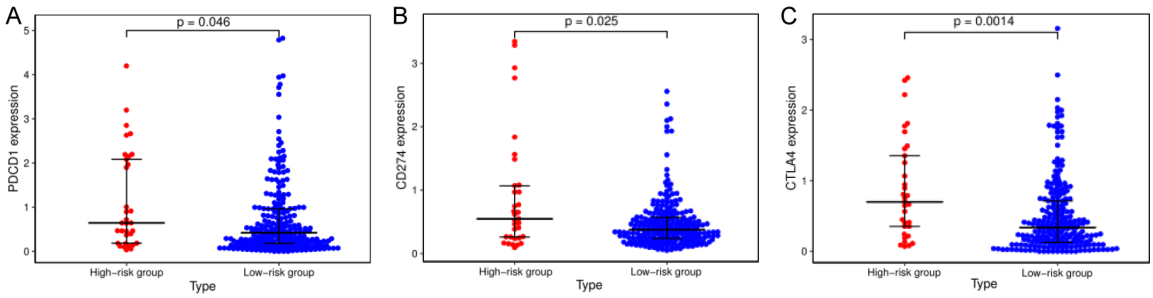

Figure 11. Scatter plots visualizing significantly different immune checkpoints between high-risk and low-risk groups. A: PDCD1. B: CD274. C: CTLA4.

correlation with the risk score (**Figure 10E**, **10F**).

Immune checkpoints expression in high and low risk groups

There were significantly elevated levels of program death 1 (PD-1), programmed death ligand 1 (PD-L1), and cytotoxic T-lymphocyte-associated protein 4 (CTLA-4) in the high-risk group compared to the low-risk group ($P < 0.05$) (**Figure 11A-C**). These findings suggest a potential influence of aberrant VI on the tumor microenvironment in the high-risk group, which may contribute to the unfavorable prognosis in these patients.

Discussion

Recently, increasing researchers have explored prognostic models of HCC. HCC patients with VI tend to have a shorter survival period. Due to the limited efficacy of current treatment approaches for VI, there is an urgent need to identify novel molecular biomarkers that can accurately predict HCC prognosis and guide

anticancer therapies. Previous studies have mainly focused on the role of single genes in VI, with limited investigation into prognostic models [10-12]. Zhou developed a prognostic model for HCC with portal vein tumor thrombosis using 5 immune-related genes; however, the model lacks validation, as well as calibration and DCA [13]. To provide a thorough evaluation of VI risk, this study utilized extensive data and complex algorithms. We performed detailed bioinformatics analyses and identified 7 genes associated with VI, namely HSPA8, ABCF2, EAF1, MARCO, EPS8L3, PLA2G1B, and C6. Subsequently, we developed a risk scoring model utilizing these genes to predict the likelihood of VI. Notably, our model exhibits the ability to differentiate between individuals at high risk and low risk, providing precise prognostic assessments.

In our study, 7 VI-related genes were used to predict the prognosis of HCC. The correlation between these genes and HCC has been documented in existing literature. HSPA8, a member of the heat shock protein family A (Hsp70), has been found to be highly expressed in HCC, and its elevated expression levels have been linked to poorer OS in patients. HSPA8 shows potential to be a prognostic biomarker in the diagnosis and treatment of HCC [14]. ABCF2, a gene encoding a member of the ATP-binding cassette (ABC) transporter superfamily, has been implicated in potential involvement in multidrug resistance. The ABCF2 gene has been identified as a target of miR-122, and its inhibition is believed to contribute to the anticancer effect of miR-122 in HCC. These findings suggest that targeting ABCF2 may have a suppressive effect on cancer progression [15]. The expression of MARCO was found to be markedly reduced in intratumoral tissues of HCC and decreased in conjunction with tumor advancement. It is noteworthy that patients with high intratumoral MARCO expression exhibited a significantly improve OS [16]. This observation contradicts our research results, with the discrepancy likely stemming from the sample size utilized in the study. EAF1 has been identified as a tumor suppressor in the mouse prostate [17], while its role in HCC remains unexplored. EPS8L3 has been found to be upregulated in liver cancer tissues and cell lines, with high expression correlating with poorer survival. EPS8L3 is implicated as an oncogene in liver cancer progression and may serve as a valuable prognostic indicator for HCC [18]. PLA2G1B, a member of phospholipase A2 group IB, has been observed to be significantly overexpressed in HCC tissue. This upregulation is found to correlate with a poorer prognosis of HCC and contribute to the construction of a prognostic model incorporating genes related to lipid metabolism in HCC [19]. C6, a complement protein involved in the formation of membrane attack complex, has been associated with improved disease-free survival and progression-free survival in HCC patients [20]. Our study supported its protective role in HCC, aligning with previous research findings. The ROC curve and calibration curve of our model illustrated its strong discriminatory power and calibration. The DCA suggests that the model holds clinical value.

Particularly, the risk score can effectively distinguish between high-risk and low-risk populations, providing precise prognostic estimates. In both the training and validation cohorts, HCC patients in the low-risk group demonstrated significantly longer OS compared to those in the high-risk group. Univariate and multivariate Cox regression analyses confirmed the risk score as an independent prognostic factor.

Our signatures demonstrated positive correlations with the infiltration levels of four immune cells, particularly neutrophils and macrophages, indicating a high level of infiltration of these cells in high-risk cases.

Within the tumor microenvironment, research has increasingly shown the crucial roles of tumor-associated neutrophils (TANs) and tumor-associated macrophages (TAMs) in infiltrating tumor tissues to facilitate growth, invasion, angiogenesis, and metastasis across different types of cancers [21, 22]. TANs and TAMs play a role in regulating molecules that facilitate angiogenesis and pro-tumor factors, such as VEGF and MMP9 [23, 24].

Furthermore, our analysis included an evaluation of immune checkpoint expression in low-risk and high-risk HCC cases. The results indicated a significant upregulation of PD-1, PD-L1, and CTLA-4 expression in high-risk HCC patients compared to their low-risk counterparts. These findings suggest that immune

checkpoint inhibitor therapy may be more effective in treating high-risk HCC cases. Prior research has investigated the relationship between PDL1 and tumor VI. Specially, PD-L1 expression in MSI-H colorectal cancers has been shown to have a strong association with poor differentiation, lymphatic invasion, and VI [25]. Furthermore, elevated serum levels of PD-L1 have been linked to advanced stages of HCC and increased mortality risk [26]. Additionally, PD-L1 has been observed to interact with vascular endothelial growth factor receptor-2 and activate the FAK/AKT pathway, leading to angiogenesis and tumor progression [27].

Nevertheless, it is essential to acknowledge some limitations within this study. This study mainly focused on bioinformatics analysis, with an absence of mechanism validation. Additional in vitro and in vivo experimental investigations are warranted to explore the precise impact of these genes on the pathogenesis of HCC. Our further endeavors will be dedicated to further elucidating the specific mechanisms underlying the role of these genes in HCC.

Conclusion

In conclusion, this study effectively developed and verified a prognostic signature consisting of 7 VI-related genes for the prognostic prediction of HCC. This prognostic signature has the capability to aid in the identification of individualized treatment strategies in clinical setting. Additionally, our risk score model establishes a correlation between VI and immune status, providing a comprehensive view for understanding the underlying mechanisms impacting HCC prognosis.

Disclosure of conflict of interest

None.

Address correspondence to: Wei-Dong Wang, Department of Interventional Radiology, The Affiliated Wuxi People's Hospital of Nanjing Medical University, Wuxi People's Hospital, Wuxi Medical Cencer, Nanjing Medical University, No. 299, Qingyang Road, Wuxi 214000, Jiangsu, China. Tel: +86-0510-85350121; E-mail: wdoc@sina.com

References

[1] Sung H, Ferlay J, Siegel RL, Laversanne M, Soerjomataram I, Jemal A and Bray F. Global cancer statistics 2020: GLOBOCAN estimates of incidence and mortality worldwide for 36 cancers in 185 countries. CA Cancer J Clin 2021; 71: 209-249.

[2] Liu Y, Li Y, Gao F, Zhang Q, Yang X, Zhu B, Niu S, Huang Y, Hu Y, Li W and Wang X. Comparison of transcatheter arterial chemoembolization-radiofrequency ablation and transcatheter arterial chemoembolization alone for advanced hepatocellular carcinoma with macrovascular invasion using propensity score analysis: a retrospective cohort study. J Oncol 2020; 2020: 1341863.

[3] Forner A, Reig M and Bruix J. Hepatocellular carcinoma. Lancet 2018; 391: 1301-1314.

[4] Thuluvath PJ. Vascular invasion is the most important predictor of survival in HCC, but how do we find it. J Clin Gastroenterol 2009; 43: 101-102.

[5] Ünal E, İdilman İS, Akata D, Özmen MN and Karçaaltıncaba M. Microvascular invasion in hepatocellular carcinoma. Diagn Interv Radiol 2016; 22: 125-132.

[6] Mínguez B, Hoshida Y, Villanueva A, Toffanin S, Cabellos L, Thung S, Mandeli J, Sia D, April C, Fan JB, Lachenmayer A, Savic R, Roayaie S, Mazzaferro V, Bruix J, Schwartz M, Friedman SL and Llovet JM. Gene-expression signature of vascular invasion in hepatocellular carcinoma. J Hepatol 2011; 55: 1325-31.

[7] Budhu A, Forgues M, Ye QH, Jia HL, He P, Zanetti KA, Kammula US, Chen Y, Qin LX, Tang ZY and Wang XW. Prediction of venous metastases, recurrence, and prognosis in hepatocellular carcinoma based on a unique immune response signature of the liver microenvironment. Cancer Cell 2006; 10: 99-111.

[8] Barrett T, Wilhite SE, Ledoux P, Evangelista C, Kim IF, Tomashevsky M, Marshall KA, Phillippy KH, Sherman PM, Holko M, Yefanov A, Lee H, Zhang N, Robertson CL, Serova N, Davis S and Soboleva A. NCBI GEO: archive for functional genomics data sets--update. Nucleic Acids Res 2013; 41: D991-995.

[9] Li T, Fan J, Wang B, Traugh N, Chen Q, Liu JS, Li B and Liu XS. TIMER: a web server for comprehensive analysis of tumor-infiltrating immune cells. Cancer Res 2017; 77: e108-e110.

[10] Guo ZY and Zhu ZT. NCAPG is a prognostic biomarker associated with vascular invasion in hepatocellular carcinoma. Eur Rev Med Pharmacol Sci 2021; 25: 7238-7251.

[11] Kurokawa T, Yamazaki S, Mitsuka Y, Moriguchi M, Sugitani M and Takayama T. Prediction of vascular invasion in hepatocellular carcinoma by next-generation des-r-carboxy prothrombin. Br J Cancer 2016; 114: 53-58.

[12] Gu J, Xu S, Chen X, Luo H, Tan G, Qi W, Ling F, Wang C, Maimaiti F, Chen Y, Yang L, Yin M and Chen D. ORM 1 as a biomarker of increased

vascular invasion and decreased sorafenib sensitivity in hepatocellular carcinoma. Bosn J Basic Med Sci 2022; 22: 949-958.
[13] Zhou W, Fang DL and He Y. Screening potential prognostic biomarkers for portal vein emboli in patients with hepatocellular carcinoma. J Gastrointest Oncol 2021; 12: 1927-1938.
[14] Wang B, Lan T, Xiao H, Chen ZH, Wei C, Chen LF, Guan JF, Yuan RF, Yu X, Hu ZG, Wu HJ, Dai Z and Wang K. The expression profiles and prognostic values of HSP70s in hepatocellular carcinoma. Cancer Cell Int 2021; 21: 286.
[15] Yahya SMM, Fathy SA, El-Khayat ZA, El-Toukhy SE, Hamed AR, Hegazy MGA and Nabih HK. Possible role of microRNA-122 in modulating multidrug resistance of hepatocellular carcinoma. Indian J Clin Biochem 2018; 33: 21-30.
[16] Sun H, Song J, Weng C, Xu J, Huang M, Huang Q, Sun R, Xiao W and Sun C. Association of decreased expression of the macrophage scavenger receptor MARCO with tumor progression and poor prognosis in human hepatocellular carcinoma. J Gastroenterol Hepatol 2017; 32: 1107-1114.
[17] Pascal LE, Su F, Wang D, Ai J, Song Q, Wang Y, O'Malley KJ, Cross B, Rigatti LH, Green A, Dhir R and Wang Z. Conditional deletion of Eaf1 induces murine prostatic intraepithelial neoplasia in mice. Neoplasia 2019; 21: 752-764.
[18] Li P, Hu T, Wang H, Tang Y, Ma Y, Wang X, Xu Y and Chen G. Upregulation of EPS8L3 is associated with tumorigenesis and poor prognosis in patients with liver cancer. Mol Med Rep 2019; 20: 2493-2499.
[19] Hu B, Yang XB and Sang XT. Construction of a lipid metabolism-related and immune-associated prognostic signature for hepatocellular carcinoma. Cancer Med 2020; 9: 7646-7662.
[20] Qian X, Yang Z, Gao L, Liu Y and Yan J. The role of complement in the clinical course of hepatocellular carcinoma. Immun Inflamm Dis 2022; 10: e569.
[21] Coffelt SB, Lewis CE, Naldini L, Brown JM, Ferrara N and De Palma M. Elusive identities and overlapping phenotypes of proangiogenic myeloid cells in tumors. Am J Pathol 2010; 176: 1564-76.
[22] Coffelt SB, Wellenstein MD and de Visser KE. Neutrophils in cancer: neutral no more. Nat Rev Cancer 2016; 16: 431-446.
[23] Dirkx AE, Oude Egbrink MG, Wagstaff J and Griffioen AW. Monocyte/macrophage infiltration in tumors: modulators of angiogenesis. J Leukoc Biol 2006; 80: 1183-96.
[24] Liang W and Ferrara N. The complex role of neutrophils in tumor angiogenesis and metastasis. Cancer Immunol Res 2016; 4: 83-91.
[25] Korehisa S, Oki E, Iimori M, Nakaji Y, Shimokawa M, Saeki H, Okano S, Oda Y and Maehara Y. Clinical significance of programmed cell death-ligand 1 expression and the immune microenvironment at the invasive front of colorectal cancers with high microsatellite instability. Int J Cancer 2018; 142: 822-832.
[26] Finkelmeier F, Canli Ö, Tal A, Pleli T, Trojan J, Schmidt M, Kronenberger B, Zeuzem S, Piiper A, Greten FR and Waidmann O. High levels of the soluble programmed death-ligand (sPD-L1) identify hepatocellular carcinoma patients with a poor prognosis. Eur J Cancer 2016; 59: 152-159.
[27] Yang Y, Xia L, Wu Y, Zhou H, Chen X, Li H, Xu M, Qi Z, Wang Z, Sun H and Cheng X. Programmed death ligand-1 regulates angiogenesis and metastasis by participating in the c-JUN/VEGFR2 signaling axis in ovarian cancer. Cancer Commun (Lond) 2021; 41: 511-527.